Bioorganic & Medicinal Chemistry Letters 19 (2009) 773–777

Contents lists available at ScienceDirect

Bioorganic & Medicinal Chemistry Letters

journal homepage: www.elsevier.com/locate/bmcl

Discovery of potent inhibitors of interleukin-2 inducible T-cell kinase (ITK) through structure-based drug design

Brian N. Cook [a,*], Jörg Bentzien [a], Andre White [a], Peter A. Nemoto [a], Ji Wang [a], Chuk C. Man [a], Fariba Soleymanzadeh [a], Hnin Hnin Khine [b], Mohammed A. Kashem [c], Stanley Z. Kugler Jr. [c], John P. Wolak [c], Gregory P. Roth [a,†], Stéphane De Lombaert [a], Steven S. Pullen [b], Hidenori Takahashi [a]

[a] Medicinal Chemistry, Boehringer Ingelheim Pharmaceuticals, Inc., 900 Ridgebury Road, PO Box 368, Ridgefield, CT 06877, USA
[b] Immunology and Inflammation, Boehringer Ingelheim Pharmaceuticals, Inc., 900 Ridgebury Road, PO Box 368, Ridgefield, CT 06877, USA
[c] Biomolecular Screening, Boehringer Ingelheim Pharmaceuticals, Inc., 900 Ridgebury Road, PO Box 368, Ridgefield, CT 06877, USA

ARTICLE INFO

Article history:
Received 21 October 2008
Revised 3 December 2008
Accepted 4 December 2008
Available online 10 December 2008

Keywords:
Kinase
Structure-based drug design
ITK
Tec kinase
SAR
Inhibitor
Benzimidazole

ABSTRACT

Interleukin-2 inducible T-cell kinase (ITK) is a member of the Tec kinase family and is involved with T-cell activation and proliferation. Due to its critical role in acting as a modulator of T-cells, ITK inhibitors could provide a novel route to anti-inflammatory therapy. This work describes the discovery of ITK inhibitors through structure-based design where high-resolution crystal structural information was used to optimize interactions within the kinase specificity pocket of the enzyme to improve both potency and selectivity.

Interleukin-2 inducible T-cell kinase (ITK) is a member of the Tec family of non-receptor tyrosine kinases which has been found to play an important role in T-cell activation and proliferation.[1] ITK is expressed primarily in T-cells, NK cells, and mast cells. Upon stimulation of the T-cell receptor (TCR), ITK is activated and serves to amplify the TCR signaling cascade.[2] Murine $CD4^+$ T-cells lacking Itk showed reduced IL-2, IL-4, IL-5, and IL-13 production upon T-cell receptor stimulation.[3–5] ITK therefore represents a novel potential target for anti-inflammatory therapy in a variety of indications such as psoriasis and allergic asthma.[6]

We have recently reported on the identification of a structurally new lead series[7] and initial optimization studies[8] that culminated in a number of acylated 2-aminobenzimidazoles, represented here by compound **1** shown in Figure 1. Compound **1** displayed good potency in a DELFIA-based molecular assay[7] (IC_{50} = 180 nM) and moderate cellular potency (IC_{50} = 2.3 μM), as measured in a stably transfected, Itk-expressing DT40 cell line assay.[7] This series of compounds was tested for selectivity against insulin receptor tyrosine kinase (IRK), an enzyme with close structural homology to ITK. Unsubstituted analogs such as compound **1** displayed poor selectivity with an IRK IC_{50} of 560 nM. A series of substituted phenyl analogs showed good selectivity and improved potency, yet still displayed modest cellular potency.[8] Therefore, we focused our optimization effort on increasing the molecular and cellular potency of the lead series, while concomitantly maintaining or improving its selectivity over IRK and other related kinases.

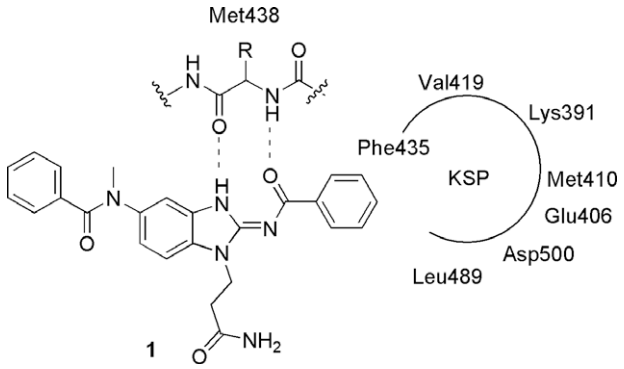

Figure 1. The structure and binding mode of **1** in ITK.

* Corresponding author. Tel.:+1 203 798 5730.
E-mail address: brian.cook@boehringer-ingelheim.com (B.N. Cook).
† Present address: Burnham Institute for Medical Research at Lake Nona, Orlando, FL 32819, USA.

0960-894X/$ - see front matter © 2009 Elsevier Ltd. All rights reserved.
doi:10.1016/j.bmcl.2008.12.028

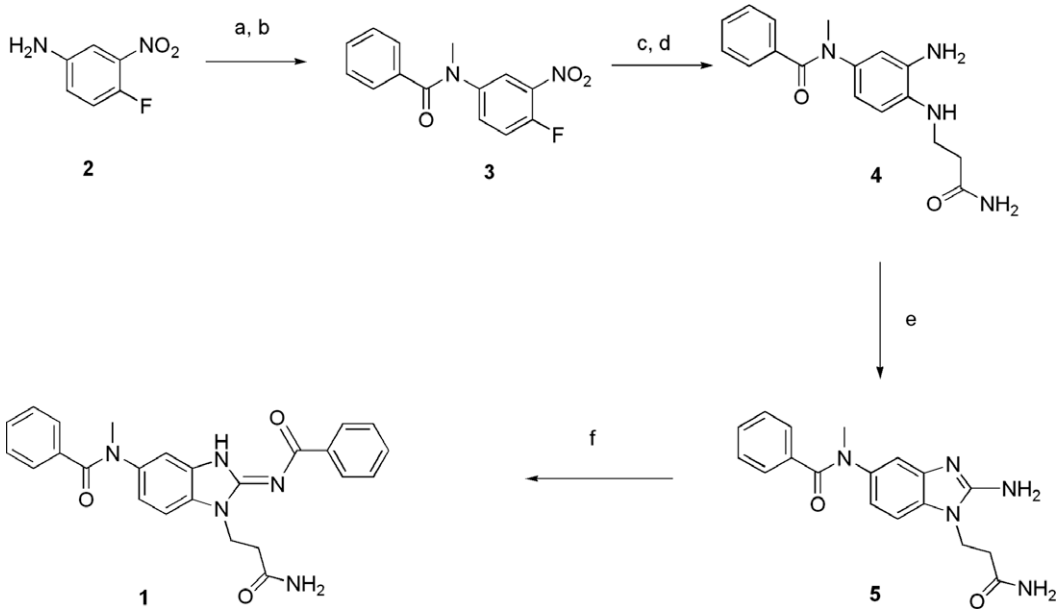

Scheme 1. General method for synthesis of 2-aminobenzimidazoles. Reagents and conditions: (a) benzoyl chloride, pyridine, CH_2Cl_2, 0 °C–rt; (b) CH_3I, NaH, THF rt, 24 h; (c) 3-aminopropanamide, DIEA, CH_3CN, 50 °C, 24 h; (d) Pd/C, H_2, CH_3OH; (e) BrCN, EtOH; rt, 24 h; (f) benzoic acid, EDCI, DIEA, DMF, rt, 24 h.

Structure-based drug design offered an appealing opportunity towards that end. Indeed, crystallographic information revealed a number of new potential interactions that could be gained.[9] Of particular interest is a vacant kinase specificity pocket (KSP) adjacent to the ATP binding site. This pocket is analogous to other reported KSPs,[10] which have been successfully exploited to yield a substantial increase in both potency and selectivity with other kinase inhibitors.[11] Access to this pocket is restricted by Phe435 which serves as a gatekeeper residue.[9] Previous reports suggest that gatekeeper residue interactions are a route to increase both potency and selectivity, as this residue often varies between disparate kinases.[12] Within the pocket, there exists a variety of functional groups that could be exploited to increase potency, such as the conformationally flexible Lys391, Glu406 (which makes up part of the distal surface of the pocket), and DGF motif loop at the bottom portion of the pocket (Asp500, Gly501, Phe502). This is in stark contrast to the lipophilic nature of the majority of KSPs described in the literature.[10] Based on the available crystallographic information, it appeared that placement of the appropriate functionality within the KSP should significantly increase binding potency.

The acylated 2-aminobenzimidazole lead series displays a somewhat unique binding motif to the hinge region of ITK. The double bond of the benzimidazole core exists as the exo-tautomer as supported by both NMR NOE studies in solution and X-ray crystallography of the molecule in complex with the ITK protein.[7–9] Two hydrogen bonds are observed between Met438 in the hinge region of the peptide backbone and the benzimidazole ring N–H as well as the acyl carbonyl oxygen. The tautomerization of the benzimidazole ring is critical for high affinity ITK binding for this series, as compounds lacking either of the H-bonding components were found to show no activity against ITK.[7,9] Critical to establishing the proper H-bonding interactions through the exo-tautomer is the aryl substituent on the right hand side of the molecule. Replacement of this aryl group with a simple alkyl or cycloalkyl group provided compounds that do not exist as the requisite tautomers (as observed by NOE) and, therefore, lack any measurable ITK inhibitory activity.[7]

Among several approaches devised to access the vacant KSP,[13] this work describes a lead optimization strategy specifically aimed at achieving this goal via a biaryl binding motif.

The general synthetic route is shown in Scheme 1. The commercially available 4-methyl-3-nitro-aniline (**2**) was acylated with benzoyl chloride and then *N*-alkylated through treatment with NaH and methyl iodide. Amine containing side-chains were introduced through S_NAr displacement of the activated aromatic fluoride **3**, and the nitro group was then reduced quantitatively to yield diamino compound **4**. Dianiline **4** was treated with cyanogen bromide to provide the 2-aminobenzimidazole **5**, which was acylated using standard conditions to provide the desired ITK inhibitors. The various carboxylic acids used were synthesized through standard methods.

Our initial attempt to improve the potency of compound **1** was focused on substitution of the phenyl ring. Of particular importance was substitution at the 4-position, as modeling suggested it would most likely point towards the Phe435 gatekeeper and the unoccupied KSP.

Small substituents at the 4-position increased both potency and selectivity, as observed previously[8] and in agreement with the molecular modeling prediction. Since the corresponding gatekeeper residue in IRK is a Met residue, it is hypothesized that the increase in selectivity over IRK results from unfavorable steric interactions at the 4-position. Interestingly, large groups, such as a phenyl ring, are not tolerated at the 4-position (compound **10**), again likely due to the position of the gatekeeper residue. However, the potencies of compounds **11** and **12** suggest that substitution at the 3-position may avoid the unfavorable Phe435 interaction, thereby providing a route around the gatekeeper residue and into the KSP (Table 1).

Based on these results, a number of other 3-substituted phenyl analogues were designed and synthesized. Unfortunately, none of those compounds showed a significant increase in potency (data not shown). Therefore, a series of heterocyclic derivatives were considered to find alternatives for the phenyl group of **1**. We reasoned that 5-membered ring heterocycles could present a unique opportunity to achieve bonding angles similar to biphenyl analogue **11**, while offering access to the KSP, around the gatekeeper residue. The 2-substituted thiophene analog had already been shown during the hit-to-lead phase to be a potent ITK inhibitor.[7] Other simple unsubstituted heterocycle analogues were explored first to determine if they would serve as effective phenyl replacements (Table 2).

Table 1
RHS aryl SAR

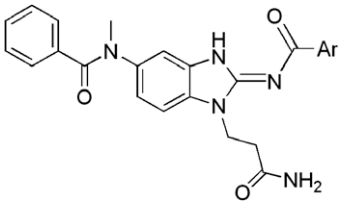

Compound	Ar	ITK IC_{50} (μM)	IRK IC_{50} (μM)	DT40 IC_{50} (μM)
1	Phenyl	0.18	0.56	2.3
6	4-Cl-phenyl	0.018	5.6	1.3
7	4-CN-phenyl	0.017	>6.0	0.33
8	4-OMe-phenyl	0.17	>6.0	>5.0
9	4-Br-phenyl	0.026	>6.0	0.73
10	4-Biphenyl	>10	>6.0	>5.0
11	3-Biphenyl	1.0	>6.0	0.09
12	1-Naphthyl	2.5	5.8	>5.0
13	2-Naphthyl	0.095	>6.0	0.54

Table 2
RHS aryl replacement SAR

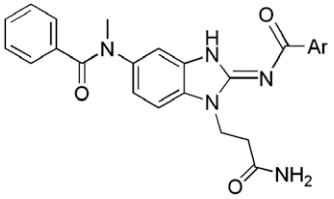

Compound	Ar	ITK IC_{50} (μM)	IRK IC_{50} (μM)	DT40 IC_{50} (μM)
1	Phenyl	0.18	0.56	2.3
14	2-Thiophene	0.058	0.15	2.7
15	3-Thiophene	0.057	0.24	1.6
16	4-Thiazole	0.34	6.1	>5.0
17	5-Thiazole	0.13	1.6	>5.0
18	2-Oxazole	0.45	>6.0	>5.0
19	4-Oxazole	0.17	>6.0	>5.0
20	5-Oxazole	0.18	>6.0	>5.0
21	5-Isoxazole	0.10	>6.0	>5.0

As observed previously,[7] the thiophene group served as a good replacement of the phenyl group, resulting in a compound of increased potency. The other heterocycles tested showed a relatively flat SAR in terms of ITK potency, although increased IRK selectivity was usually observed. We hypothesized that this could again result from unfavorable interactions (perhaps electrostatic in nature) with the IRK Met gatekeeper residue. Since substitution of the thiophene would allow for presentation of other groups at angles distinct from the corresponding phenyl analogs, the 2,5-disubstituted thiophene was chosen as a scaffold for further optimization as shown in Table 3.

Substitution at the 5-position of the thiophene ring was found to increase potency dramatically. Simple halogen substitution, as in **22** and **23**, increased molecular potency 4-fold, with similar gains observed in cellular potency. Cyano substitution at the 5-position also enhanced potency, while providing a 250-fold selectivity for ITK over IRK (see compound **24**). Appending a 5-formyl group provided the highly potent compound **25**, likely though formation of a covalent intermediate with Lys391. In follow-up experiments, incubation of the enzyme with compound **25** in the presence of a reducing agent showed formation of the irreversible Lys391 adduct, supporting the formation of a Schiff's base intermediate. To a lesser extent, the ketone containing compounds **26**–**28** may also interact with the Lys391 residue. These compounds show improved selectivity against IRK, however, likely due to the distinct steric requirements of the gatekeeper residues in the different active sites.

Table 3
RHS 5-thienyl substitution SAR

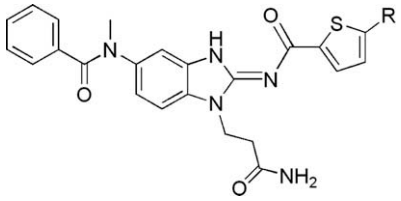

Compound	R	ITK IC_{50} (μM)	IRK IC_{50} (μM)	DT40 IC_{50} (μM)
14	H	0.058	0.15	2.7
22	Cl	0.014	0.38	0.52
23	Br	0.015	0.63	0.10
24	CN	0.015	3.8	0.15
25	CHO	0.002	0.051	0.02
26	$COCH_3$	0.014	>6.0	0.39
27	$COCH(CH_3)_2$	0.020	>6.0	0.57
28	COPh	0.055	>6.0	0.15
29	OPh	0.14	>6.0	0.47
30	OBn	0.035	>6.0	1.2
31	Ph	0.039	>6.0	0.82
32	2-Pyr	0.019	>6.0	0.65
33	3-Pyr	0.005	>6.0	0.04
34	4-Pyr	0.002	>6.0	0.51

Aryl substitution (examples **31**–**34**) was tolerated at the 5-position, confirming that the 5-position of the thiophene offered a beneficial presentation of functionality which avoided the Phe435 gatekeeper residue. Of particular significance was the dramatic increase in molecular and cellular potency of the 3- and 4-pyridine functionalized compounds. Introduction of the 2-pyridyl motif (**32**) did not result in a substantial increase in potency as compared to the phenyl analogue **31**. However, both the 3- and 4-pyridyl analogues **33** and **34** (respectively) showed much improved molecular potency, with similar gains observed in the cellular assay for **33**. In addition, these compounds displayed very good selectivity against IRK.

A co-crystal structure of compound **32** with ITK was obtained, providing insights about the interactions within the KSP. As shown in Figure 2, the 2-pyridyl moiety of **32** may benefit from a hydrophobic π-stacking interaction with the gatekeeper Phe435, which is absent in the IRK active site. In addition, the pyridine ring points directly into the vacant selectivity pocket. From the structure, the 2-pyridine does not appear to pick up any additional interactions. However, compounds **33** and **34** may be able to engage in hydrogen bonding interactions with either Lys391 or Asp500, resulting in the increased potencies observed.

Based on these results, the thiophene biaryl inhibitors were further modified through the introduction of pendant heterocyclic replacements of the pyridine motif of **32**–**34** (Table 4). The various oxazole analogues showed good potency when assayed against ITK, with the 5-oxazole being the most potent. This compound overlaps nicely with the 3-pyridyl analogue **33** which was previously observed to impart high potency. The 2- and 4-oxazoles displayed reduced activity, similar to 2-pyridyl analogue **32**, again suggesting that opportunities for H-bonding interactions exist deep within the KSP. All other nitrogen containing aromatic heterocycles were potent ITK inhibitors, while saturated analogues **43**–**46** were weaker. This loss of potency was attributed to a lack of a π-stacking interaction with Phe435, or unfavorable electro-

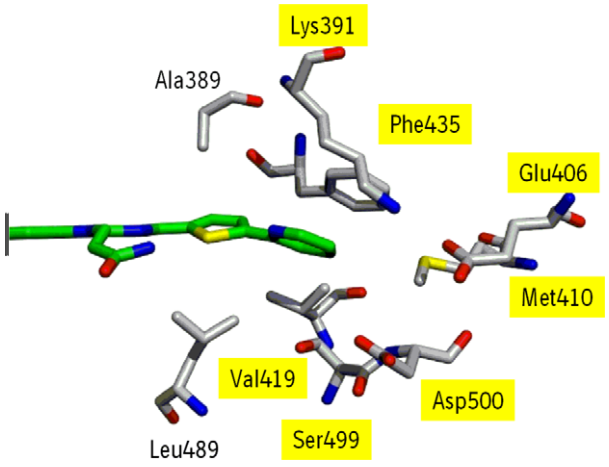

Figure 2. The X-ray crystal structure of **32** and interactions in the KSP of ITK.

static repulsion between Lys391 and the protonated basic amine (or oxygen heteroatom) in the saturated ring system.

Interestingly, pyrazole analogue **41** was the most potent compound tested in the cellular assay, with an IC_{50} of 2 nM. It was 25-fold more potent than 5-oxazole analogue **37**) even though they displayed similar molecular potency under the assay conditions. Based on the conditions used for the molecular assay, the predicted assay range does not extend below 2 nM. Therefore, we developed an assay with a higher concentration of ATP to extend the dynamic range of the assay, thereby allowing for the direct comparison of the most potent of inhibitors. Additional analogues containing the pyrazole and 5-oxazole moieties were synthesized with various groups appended from the 1-position of the benzimidazole to improve physicochemical properties of the molecules. When these analogues were tested in the higher ATP concentration assay, the pyrazole analogues were found to be consistently 10-fold more potent than the corresponding oxazole analogues. This finding supports the cellular potency increase observed in the case of pyrazole analogue **41**. Molecular modeling suggests that the pyrazole is able to form two distinct hydrogen bonds within the KSP: one with Lys391 and the other with Asp500. In addition, the T-shaped orientation of the heterocycle and the aryl ring of Phe435 can provide a favorable interaction (Fig. 3 below). In contrast, the oxazole analogue occupies a similar space, but only benefits from a single hydrogen bond interaction with Lys391.

Table 4
RHS 5-thienyl substitution SAR

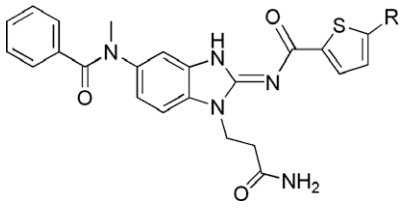

Compound	R	ITK IC_{50} (μM)	IRK IC_{50} (μM)	DT40 IC_{50} (μM)
35	2-Oxazole	0.008	>6.0	0.10
36	4-Oxazole	0.014	>6.0	0.74
37	5-Oxazole	0.002	5.2	0.05
38	2-Me-5-oxazole	0.006	2.4	0.06
39	2-Thiazole	0.011	>6.0	0.19
40	2-Amino-4-Thiazole	0.010	>6.0	1.3
41	4-Pyrazole	0.002	2.0	0.002
42	2-Pyrazine	0.013	>6.0	0.73
43	Pyrrolidine	0.081	>6.0	1.8
44	Piperidine	0.38	>6.0	>3.2
45	Piperazine	0.15	>6.0	>3.2
46	4-Morpholine	0.074	>6.0	>3.2
47	2-CN-4-pyridine	0.008	>6.0	0.09
48	2-F-4-pyridine	0.003	>6.0	0.06
49	2-CN-5-pyridine	0.010	>6.0	0.26
50	2-F-5-pyridine	0.005	>6.0	0.19
51	3-CN-5-pyridine	0.002	>6.0	0.10

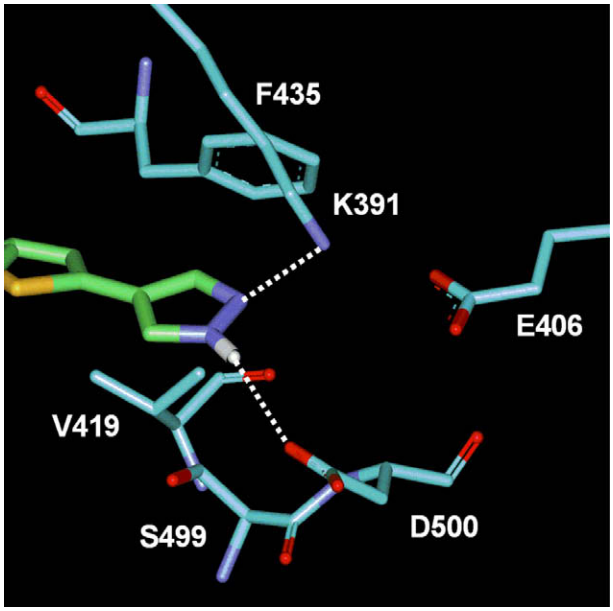

Figure 3. The molecular modelling structure and binding mode of pyrazole compound **41** in the KSP. Two possible H-bond interactions are observed to K391 and D500.

Both the oxazole and pyrazole derivatives showed greater than 1000-fold selectivity over IRK. This is in stark contrast to lead compounds **1** and **14**, which each showed approximately 3-fold selectivity. In addition, the cellular potency of the biaryl compounds was increased more than 1000-fold over the unsubstituted thiophene inhibitor **14**.

In summary, a series of biaryl thiophene-containing ITK inhibitors was identified. These compounds were designed to avoid the gatekeeper Phe residue and occupy the vacant KSP of ITK to increase potency and selectivity against IRK. Molecular modeling as well as X-ray crystallography guided molecule design and led to ITK inhibitors that showed a greater than 100-fold increase in molecular potency and a coincident 1000-fold increase in cellular potency. In addition, selectivity for ITK inhibition over IRK was increased from 3-fold to greater than 1000-fold. Notably, compound **41** is the most potent ITK inhibitor reported to date. Further details regarding the in vivo efficacy of these biaryl-containing ITK inhibitors will be presented in forthcoming publications.

References and notes

1. (a) Kane, L. P.; Lin, J.; Weiss, A. *Curr. Opin. Immunol.* **2000**, *12*, 242; (b) Samelson, L. E. *Annu. Rev. Immunol.* **2002**, *20*, 371; (c) Ohashi, P. S. *Nat. Rev. Immunol.* **2002**, *2*, 427.
2. Lin, T. A.; McIntyre, K. W.; Das, J.; Liu, C.; O'Day, K. D.; Penhallow, B.; Hung, C. Y.; Whitney, G. S.; Shuster, D. J.; Yang, X.; Townsend, R.; Postelnek, J.; Spergel, S. H.; Lin, J.; Moquin, R. V.; Furch, J. A.; Kamath, A. V.; Zhang, H.; Marathe, P. H.; Perez-Villar, J. J.; Doweyko, A.; Killar, L.; Dodd, J. H.; Barrish, J. C.; Wityak, J.; Kanner, S. B. *Biochemistry* **2004**, *43*, 11056.

3. Schaeffer, E. M.; Yap, G. S.; Lewis, C. M.; Czar, M. J.; McVicar, D. W.; Cheever, A. W.; Sher, A.; Schwartzberg, P. L. *Nat. Immunol.* **2001**, *2*, 1183.
4. Schaefer, E. M.; Debnath, J.; Yap, G.; McVicar, D.; Liao, X. C.; Littman, D. R.; Sher, A.; Varmus, H. E.; Lenardo, M. J.; Schwartzberg, P. L. *Science* **1999**, *284*, 638.
5. Fowell, D. J.; Shinkai, K.; Liao, X. C.; Beebe, A. M.; Coffman, R. L.; Littman, D. R.; Locksley, R. M. *Immunity* **1999**, *11*, 399.
6. Forssell, J.; Sideras, P.; Eriksson, C.; Malm-Erjefalt, M.; Rydell-Tormanen, K.; Ericsson, P. O.; Erjefalt, J. S. *Am. J. Respir. Cell Mol. Biol.* **2005**, *32*, 511.
7. Snow, R. S.; Abeywardane, A.; Campbell, S.; Lord, J.; Kashem, M. A.; Khine, H. H.; King, J.; Kowalski, J. A.; Pullen, S. S.; Roma, T.; Roth, G. P.; Sarko, C. R.; Wilson, N. S.; Winters, M. P.; Wolak, J. P.; Cywin, C. L. *Bioorg. Med. Chem. Lett.* **2007**, *17*, 3660.
8. Moriarty, K. J.; Takahashi, H.; Pullen, S. S.; Khine, H. H.; Sallati, R. H.; Raymond, E. L.; Woska, J. R., Jr.; Jeanfavre, D. D.; Roth, G. P.; Winters, M. P.; Qiao, L.; Ryan, D.; DesJarlais, R.; Robinson, D.; Wilson, M.; Bobko, M.; Cook, B. N.; Lo, H. Y.; Nemoto, P. A.; Kashem, M. A.; Wolak, J. P.; White, A.; Magolda, R. L.; Tomczuk, B. *Bioorg. Med. Chem. Lett.* **2008**, *18*, 5545.
9. White, A.; Abeywardane, A.; Cook, B. N.; Fuschetto, N.; Gautschi, E.; John, A.; Kroe, R. R.; Kronkaitis, A.; Xiang, L.; Pullen, S. S.; Roma, T.; Moriarity, K. J.; Roth, G. P.; Snow, R. J.; Studts, J. M.; Takahashi, H.; Farmer, B. T., II; *J. Biol. Chem.*, submitted for publication.
10. (a) Cherry, M.; Williams, D. H. *Curr. Med. Chem.* **2004**, *11*, 663; (b) Cirillo, P. F.; Pargellis, C.; Regan, J. *Curr. Top. Med. Chem.* **2002**, *2*, 1019; Regan, J.; Breitfelder, S.; Cirillo, P.; Gilmore, T.; Graham, A. G.; Hickey, E.; Klaus, B.; Madwed, J.; Moriak, M.; Moss, N.; Pargellis, C.; Pax, S.; Proto, A.; Swinamer, A.; Tong, L.; Torcellini, C. *J. Med. Chem.* **2002**, *45*, 2994.
11. (a) Tong, L.; Pav, S.; White, D. M.; Rogers, S.; Crane, K. M.; Cywin, C. L.; Brown, M. L.; Pargellis, C. A. *Nat. Struct. Biol.* **1997**, *4*, 311; (b) Fitzgerald, C. E.; Patel, S. B.; Becker, J. W.; Cameron, P. M.; Zaller, D.; Pikounis, V. B.; O'Keefe, S. J.; Scapin, G. *Nat. Struct. Biol.* **2003**, *10*, 764; (c) Gallagher, T. F.; Fler-Thompson, S. M.; Garigipati, R. S.; Sorenson, M. E.; Smietana, J. M.; Lee, D.; Bender, P. E.; Lee, J. C.; Laydon, J. T.; Griswold, D. E.; Chabot-Fletcher, M. C.; Breton, J. J.; Adams, J. L. *Bioorg. Med. Chem. Lett.* **1995**, *5*, 1171; (d) Liverton, N. J.; Butcher, J. W.; Claiborne, C. F.; Claremon, D. A.; Libby, B. E.; Nguyen, K. T.; Pitzenberger, S. M.; Seinick, H. G.; Smith, G. R.; Tebben, A.; Vacca, J. P.; Varga, S. L.; Agarwal, L.; Dancheck, K.; Forsyth, A. J.; Fletcher, D. S.; Frantz, B.; Hanlon, W. A.; Harper, C. F.; Hofsess, S. J.; Kostura, M.; Lin, J.; Luell, S.; O'Neill, E. A.; Orevillo, C. J.; Pang, M.; Parsons, J.; Rolando, A.; Sahly, Y.; Visco, D. M.; O'Keefe, S. J. *J. Med. Chem.* **1999**, *42*, 2180.
12. (a) Noble, M. E. M.; Endicott, J. A.; Johnson, L. N. *Science* **2004**, *303*, 1800; (b) Lin, T. H.; Metzger, A.; Diller, D. J.; Desai, M.; Henderson, I.; Ahmed, G.; Kimble, E. F.; Quadros, E.; Webb, M. L. *J. Pharmacol. Exp. Ther.* **2006**, *318*, 495.
13. Lo, H. Y.; Bentzien, J.; Fleck, R. W.; Pullen, S. S.; Khine, H. H.; Woska, J. R., Jr.; Kugler, S. Z.; Kashem, M. A.; Takahashi, H. *Bioorg. Med. Chem. Lett.* **2008**, *18*, 6218; Lo, H. Y.; Bentzien, J.; White, A.; Man, C. C.; Fleck, R. W.; Pullen, S. S.; Khine, H. H.; King, J.; Woska, J. R., Jr.; Wolak, J. P.; Kashem, M. A.; Roth, G. P.; Takahashi, H. *Tetrahedron Lett.* **2008**, *49*, 7337.